Available online at www.sciencedirect.com

ScienceDirect

Physics Procedia 66 (2015) 249 – 259

Physics Procedia

C 23rd Conference on Application of Accelerators in Research and Industry, CAARI 2014

Proposed New Accelerator Design for Homeland Security X-Ray Applications

James Clayton[a], Daniel Shedlock[a], Willem G. J. Langeveld[b,]*, Vinod Bharadwaj[c], Yuri Nosochkov[c]

[a]*Varian Medical Systems, Inc., 3120 Hansen Way, Palo Alto, CA 94304, USA*
[b]*Rapiscan Laboratories, Inc., 520 Almanor Avenue. Sunnyvale, CA 94085, USA*
[c] *SLAC National Accelerator Laboratory, 2575 Sandhill Rd, Menlo Park, CA,94025 USA*

Abstract

Two goals for security scanning of cargo and freight are the ability to determine the type of material that is being imaged, and to do so at low radiation dose. One commonly used technique to determine the effective Z of the cargo is dual-energy imaging, i.e. imaging with different x-ray energy spectra. Another technique uses the fact that the transmitted x-ray spectrum itself also depends on the effective Z. Spectroscopy is difficult because the energy of individual x rays needs to be measured in a very high count-rate environment. Typical accelerators for security applications offer large but short bursts of x-rays, suitable for current-mode integrated imaging. In order to perform x-ray spectroscopy, a new accelerator design is desired that has the following features: 1) increased duty factor in order to spread out the arrival of x-rays at the detector array over time; 2) x-ray intensity modulation from one delivered pulse to the next by adjusting the accelerator electron beam instantaneous current so as to deliver adequate signal without saturating the spectroscopic detector; and 3) the capability to direct the (forward peaked) x-ray intensity towards high-attenuation areas in the cargo ("fan-beam-steering"). Current sources are capable of 0.1% duty factor, although usually they are operated at significantly lower duty factors (~0.04%), but duty factors in the range 0.4-1.0% are desired. The higher duty factor can be accomplished, e.g., by moving from 300 pulses per second (pps) to 1000 pps and/or increasing the pulse duration from a typical 4 μs to 10 μs. This paper describes initial R&D to examine cost effective modifications that could be performed on a typical accelerator for these purposes, as well as R&D for fan-beam steering.

Selection and peer-review under responsibility of the Organizing Committee of CAARI 2014

Keywords: High duty factor; accelerator; x-ray; spectroscopy; beam current modulation; material discrimination

* Corresponding author. Tel.: +1-408-961-9709; fax: +1-408-727-8748.
E-mail address: wlangeveld@rapiscansystems.com

Selection and peer-review under responsibility of the Organizing Committee of CAARI 2014
doi:10.1016/j.phpro.2015.05.032

1. Overview

In the security and inspection market, there is a push towards highly mobile, reduced-dose active interrogation scanning and imaging systems to allow operation in urban environments (Langeveld, Gozani et al., 2013). To achieve these goals, the accelerator system design needs to be smaller than existing systems and have a considerably reduced weight. A smaller radiation exclusion zone may be accomplished through better beam collimation (reduced ancillary dose field through better beam control to reduce the shielding weight as described below), and an integrated, x-ray-source/detector-array assembly to allow feedback and control of an intensity-modulated x-ray source (IMAXS, see, e.g., Langeveld, Johnson et al. 2009a and 2009b, and Langeveld, Brown et al., 2011). Transmitted x-ray spectroscopy (Z-SPEC, see, e.g., Stevenson et al., 2010, Sinha et al. 2013) and statistical waveform analysis (Z-SCAN, see e,g,, Langeveld, Condron et al. 2011 and 2013) may be used to improve material discrimination. A shaped low-Z target in the x-ray source can be used to generate a more forward peaked x-ray beam, reducing shielding weight. Electron-beam steering can then be applied to direct the forward-peaked x rays towards areas in the cargo with high attenuation, in a form of rastering. Previous R&D on high-duty-factor x-ray sources is discussed in Condron et al. (2013). Here, we describe R&D in progress on an IMAXS x-ray source with increased duty factor, improving Z-SPEC/Z-SCAN material separation performance, and R&D to achieve electron beam steering. This paper reports on an exploratory study to identify components and upgrades that would be required to meet the desired specifications, as well as the best technical approach to design and build a prototype.

Nomenclature

COTS	Commercial Off-The-Shelf
IBCM	Instantaneous Beam Current Modulation
IMAXS	Intensity Modulated Advanced X-ray Source
Linac	Linear accelerator
PRF	Pulse Rate Frequency
SLAC	SLAC National Accelerator Laboratory
Z-SPEC	Transmitted x-ray spectroscopy to determine the projected average atomic Z of the material
Z-SCAN	Projected average Z-determination by Statistical Count-rate ANalysis

2. Technical Approach

The new accelerator design has two goals. One goal is to develop a truck-mounted light-weight high-duty-factor high-energy x-ray source, the other is to develop a beam line that allows for x-ray fan-beam steering.

In order to arrive at such a new design, it is best to take a two-step approach in order to mitigate development risks. In the first step, many of the components such as the modulator, klystron, target, cooling system, accelerator wave guide, circulator and load need to be customized. This requires extensive development and testing, and thus a stable test and development environment is a prerequisite. This would simplify integration, testing, and diagnosis of the new or modified components for full functionality, before undertaking the more specific engineering task of packaging the components for a compact light-weight truck-mounted system. This demonstration system would be specifically designed for extended, stable operation for troubleshooting and easy integration of new or modified components. The new beam steering components envisioned to accomplish the second goal could also be tested and refined in the demonstration system. Additionally, new components would be developed to specifications compatible with the final goal of truck-mounted operation.

Once each of the components has been developed and fully tested in the demonstration system and the functionality has been verified, the next phase would consist of adjusting and/or re-engineering the components for a truck-mounted platform where necessary. A comparative summary of the R&D required for the demonstration system and the final truck-mounted system is given in Table 1.

Table 1 Demonstration System vs. Truck-Mounted System. A two-phase development program is indicated. Tasks shaded in orange are primary development tasks in each phase.

Component	Demonstration System (Phase I)	Truck-Mounted System (Phase II)
Superstructure	Based on existing VMS K15 frame and components.	Specific to truck-mounted system.
Shielding	Optimized shielding for target and beam line.	As is from Demonstration System, minor changes to mount points and structure.
RF guide (beam centerline)	Typical 22 MV guide with enhanced cooling.	New design with enhanced cooling optimized for 9 MeV with low beam loading.
RF network, circulator, load	COTS, but upgraded from the standard 22 MV guide.	Specific to truck-mounted environment.
240-270° magnet	COTS 270° magnet	Optimized (permanent?) magnet, perhaps at 240° or 245° rather than 270°.
Target	Low-Z, new design, for use with beam steering.	As is from Demonstration System.
Klystron	COTS, modified to higher average power, lower peak power.	Optimize PoC klystron for mobile use.
Modulator	Line-type modulator, further development of existing design.	As is from Demonstration System.
Gun	Gridded electron triode gun and high-duty-factor gun driver.	As is from Demonstration System.
Temperature control unit (TCU)	COTS TCU, but still differs from standard offering.	Multi-loop large-reservoir unit optimized for inspection system effective on-off cycle.

3. Demonstration System Overview and Goals

The design goal for the demonstration system is to provide a stable environment for development testing of new or modified components. It is oriented to fit inside the footprint of the current industrial Varian K15 platform. The K15 industrial package was selected because existing framework and housing can easily support all the accelerator system source requirements (as it shares many components with the typical 22 MV systems). With "typical 22 MV accelerator" we mean Varian's latest accelerator design, capable of electron beam energies from ~2 MeV to ~22 MeV. This accelerator system was selected as the starting point, because more components for the RF network and HV are available. The 22-MV guide also has a higher starting heat load capacity, which is needed for the high-duty-factor source. However, the accelerator section is relatively long, which would require it to be mounted vertically in an eventual mobile form factor. Therefore, the repackaged K15 setup would include a 270-degree ("alpha") bend magnet. Bend magnets from both the Varian Clinac™ and Varian TrueBeam™ systems have been evaluated. Section 3 details the proposed demonstration system, including the fan-beam steering beam line, and Section 4 discusses the evolution to a truck-mounted system in some further detail.

Reduction in size and weight would be evaluated in the second phase, once the primary accelerator components and beam steering have been demonstrated and developed. If a 1% duty factor is achieved, the average RF power of the system will be in the 9-12 kW range. The pulse rate will be increased from 300-400 Hz (today's systems) to 1000 Hz. In order to perform x-ray spectroscopy and reduce the dose, instantaneous beam current modulation by a factor of up to ~32 is desired. The first phase would involve analyzing the viability and variability of this modulation to determine whether discrete or continuous control is desirable. Analysis would be performed on the electron targets and beam center line to determine the heat load (average system power) that can be tolerated. The maximum average system power is determined by the combination of pulse rate frequency, instantaneous beam current modulation, and pulse amplitude. With a PRF of 1000 Hz, it may only be possible to achieve a pulse width of 8-10 μs with a klystron-driven system, or 2-4 μs with a magnetron-driven system. Even with these limitations, the duty cycle of the source is increased from 0.1% to ~0.3% for a magnetron-based system, and to an easily obtainable duty factor of 0.5% and highly likely achievable 1% duty factor for a klystron-based system, if all components perform to specification. The unfiltered maximum output design dose for the system of 100 Rad/min at 1 meter at 9 MV is sufficient to penetrate >32 cm of steel-equivalent during cargo inspection. If this dose rate can be achieved at lower power, then it may be possible to increase the duty factor further. The initial analysis focusses on a 9-MV S-band system with a potentially more compact X-band source envisioned in the future. A klystron-operated

source is more flexible than a magnetron-operated one, and for high duty factor, a klystron-operated source is required. While the increased power available from a klystron can also reduce the length of the Linac, we would likely trade increased Linac length for decreased power consumption to remain within the available power budget for a mobile system.

Electron-beam characteristics at the exit of the 270-degree bend magnet of our typical 22-MV Linac operating at 9 MV were calculated and used to design the beam line for the fan-beam steering system. In a fan-beam steering system, the electron beam from the Linac is bent vertically using a dipole kicker magnet, and refocused on the x-ray production target. In this way, the target point itself does not move, but the impact direction of the electron beam changes in the vertical plane. Since the x rays are produced from the target with the highest intensity in the direction of the electron beam, the highest x-ray dose can thus be concentrated on areas of the scanned object (usually cargo) with the highest areal density. In addition, the x rays are also collimated in the vertical plane, creating a fan beam profile. When a low-Z target is used, the x rays are more forward directed, allowing greater selectivity in where to apply the highest x-ray intensity to the cargo. In operation, a vertical slice of the cargo image is acquired by pulsing the x-ray source and acquiring data from the (linear) detector array. The slice is analyzed, estimating where the cargo areal density is highest, and from that the optimal electron beam angle and instantaneous beam current are determined in order to adequately image the cargo while maintaining a low dose. These settings are then applied to the next slice (or x-ray pulse), after which the process repeats until the entire cargo object is scanned. In a high-pulse-rate system, it is obviously possible to combine multiple x-ray pulses to form a single vertical slice of the image.

3.1. *K15 Frame Type Demonstration System*

The demonstration system can be built with relatively low risk and a very high probability of success when using a current commercial off-the-shelf framework such as the Varian K15. For this system, the framework and superstructure can be easily modified to support the necessary component upgrades. Either the current K15 guide, M9 guide or the 22-MV guide could be mounted in the K15 structure. The 22-MV guide has a gridded electron triode gun, as is preferred, since it can control the beam current with greater accuracy.

The RF network for the 22-MV guide operates at 2856 MHz. The RF driver for the network would need to be upgraded in order to handle the higher duty factor. The system would use a variant of CPI klystron model 8262–F or 8262-M that has an upgraded collector to handle duty factors of ~1%. The pulse width would be in the range of 8-11 μs with a pulse rate of 900-1250 kHz.

In addition, the gun driver would have to be upgraded to match the higher duty-factor (~1%) specifications. Ideally, the peak cathode current, peak grid current, and the grid bias would stay as close to "typical" settings used for cargo screening as possible. Dose rates for a mobile cargo screening applications range from 0.1 – 2 Gy/min at 1 m from the x-ray target. The gun settings are determined by the Z-SCAN and Z-SPEC imaging requirements and the leakage radiation footprint allowed at the inspection site.

Another component which requires careful consideration is the modulator. One option would be a line-type 25-kW IGBT modulator. This would use a fixed 10 μsec pulse width and the capability of operating at 1 kHz with a pulse voltage of 90 kV and pulse current of 30 A for the klystron. With this type of modulator there is no capability for pulse-to-pulse variation of the pulse width, and the system would rely on the triode gun for pulse-to-pulse beam current adjustment. The second type of modulator considered is a solid-state modulator. A solid-state modulator offers more adjustability without relying completely on the triode gun for beam current adjustment.

Both L3 and CPI can develop a klystron capable of operation at 1% duty factor with 1-1.3 MW of peak power. CPI has a commercial family of tubes that operate at 2856 MHz and that allow high average power. The 8262-F is a klystron that was developed for driving linear accelerators for medical sterilization or food irradiation. This tube is capable of 36 kW of average output power, with a duty factor of 0.72%. The 8262-M is a 3 MW klystron that has been used for Varian Medical Systems Security & Inspection Products to drive the K9 dual-energy interlaced x-ray source. It has a (standard-operation) duty factor of 0.4%. These tubes are typically designed to operate at 3 or 5.5 MW of peak power. Because the demonstration system will use around 1 MW of peak power, variants of these tubes can be designed and tuned for the demonstration system with higher duty factor at the lower peak power. They have a collector that can handle the average power, but need to be optimized for the desired output level.

These tubes will likely be less efficient than when operated in their standard operating range, at an estimated 35-40% efficiency rather than 50%, and will thus require relatively more modulator power than typical medical or industrial systems.

A four-port circulator and water load that can operate at 2856 MHz with 1.2 MW of peak power and 12 kW of average power is also needed. There are several suppliers who can provide extensions to current COTS products to meet the specification. The high power level necessary to achieve the 1% system duty factor will require significant cooling. The accelerator and circulator will require water that is temperature controlled to within $\pm 1°$ C, and ideally within $\pm$ 0.5° C. The modulator is expected to dissipate about 10-15 kW of heat which will need to be removed from the unit. The accelerator structure will dissipate another 7-10 kW of heat and the circulator and load are expected, on average, to dissipate another 1-2 kW. There will be additional loads for cooling accelerator solenoids, target, orbit chamber and energy slits. The klystron solenoid (4.5 kW), klystron body and klystron collector (10-15 kW) will also need to be cooled. One option, to keep cost and size down, is to use two water cooling systems. One temperature control unit (chiller/heater) would supply items that need water with more tightly regulated control, and the second one would have a more relaxed temperature range for operation, perhaps on the order of ± 5° C. Overall, the system would likely be run at elevated temperature in order to prevent condensation in areas where the relative humidity is high. In the mobile application, the cooling system may have to operate with ambient external temperatures that range from -40 °C to +50 °C. This will require the development of heater units for extreme cold weather and extra cooling in extreme desert-like conditions.

The K15 superstructure would need to be modified for attachment of the 270° bend magnet. This entails a straightforward mechanical modification.

The software control system would be a custom version of the current Varian Security and Inspection Products (SIP) accelerator control system. Modifications to the software would include control for fine tuning new or modified component inputs that are not available in the existing control software. A hardware and software control system for the bend magnet and tuning system as well as an interface for the fan-beam steering system would also need to be included.

The risks associated with building and testing this demonstration system are component driven. With many of the components being COTS, and the exceptions detailed above, the risks for the demonstration system are well-understood. The IBCM feature can be tested in the demonstration system as well since the electron gun is gridded which provides flexibility to change the X-ray output within the required range on a pulse to pulse basis. A conceptual sketch (not to scale) of what the demonstration system would like is shown in Fig. 1.

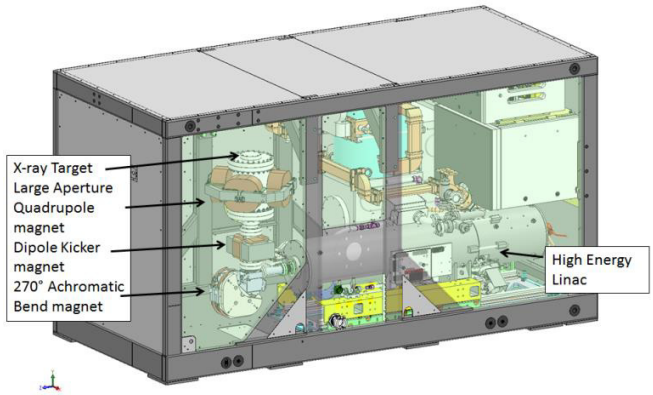

Fig. 1, Demonstration system sketch with K15 support structure, 270 degree bend magnet, large aperture quadrapole magnet, dipole kicker magnet, line type or solid state modulator with high duty.

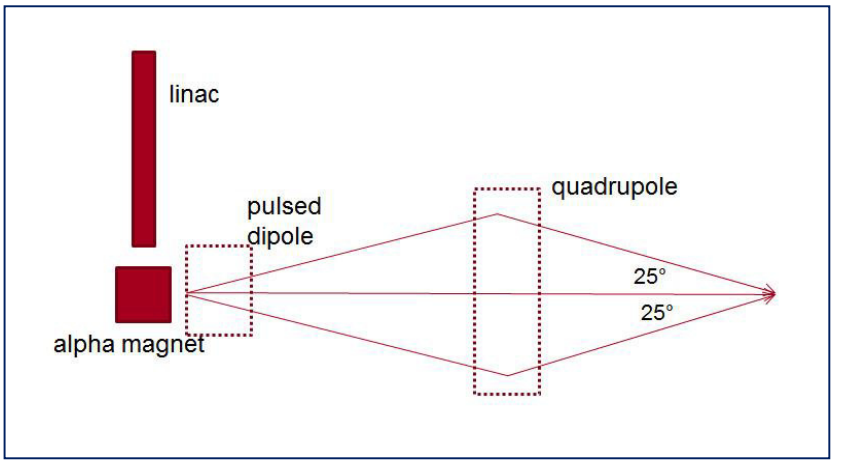

Fig. 2: Simplified electron trajectory inside the beamline

3.2. Beam transport and simulations

Parmela accelerator beam transport (Young 2003) calculations were performed and data files were created for various demonstration system configurations. These were subsequently used as input for the design of the fan-beam steering system. The fan-beam steering optics from the alpha-magnet (270°) to the x-ray production target should satisfy the following requirements:

- Total beam transport length of less than 2 feet;
- Adjustable vertical angle at the target in the range of ±25°, with no horizontal angle;
- RMS beam size at the target on the order of ~1 mm or less (more important for the vertical size);
- Stability of the beam position at the target on the order of a few mm.

Figure 2 shows a simplified concept of the beamline. The beam that comes out of the alpha magnet is steered onto the target using a pulsed dipole followed by a DC quadrupole. The pulsed dipole consists of a fast (~1 kHz) vertically deflecting kicker. The kicker creates a vertical angle on the orbit; then the resulting vertical beam trajectory is directed to the x = y = 0 position at the x-ray production target by the strongly focusing quadrupole magnet. For an ideal magnetic field and in the absence of errors, the kicker strength is linearly proportional to the angle at the target, and the quadrupole has a fixed strength, focusing the beam to the same position at the target independent of the kicker angle.

The beamline is designed to run at a nominal beam energy of 9 MeV. The driving consideration for designing this beamline is the fact that it has to be extremely short in length (~50 cm). We chose to design for a maximum dipole kick of 15° and then set the quadrupole position so as to generate the needed 25° angle at the photon target.

The pulsed dipole is designed for a kicker frequency of ~1 kHz, corresponding to the maximum anticipated Linac pulse rate. Given the beamline layout, the desired pole tip field is ~0.5 kG. A full magnet gap of 2.5 cm is sufficient to contain all the possible beam orbits in the +/–15° range. The magnet should have enough integrated strength to allow a 15° (~0.268 radians) deflection. Since overall length is at a premium, the dipole has an iron core, and is laminated to minimize eddy currents and excessive heating. The core steel should be a grain-oriented silicone steel or equivalent. This magnet is designated as a "1D3.5" magnet (i.e. a dipole with 1" gap and 3.5" core length), and has an expected effective magnetic length of ~4" (10 cm). The required integrated strength is ~88 Gm which implies a pole tip field of 0.88 kG. The number of ampere-turns to drive this flux is ~1780. For an assumed excitation current of 5 A, we will need ~360 turns, or 180 turns per pole. We would use AWG #12 conductor, which is small enough that we do not need a multi-stranded wire to minimize eddy current losses in the coil. The sagitta will be ~3.33 mm and the 3-inch wide pole configuration will provide enough good field region to allow deflections in both directions from the magnet center. The dipole design is shown in Fig. 3a.

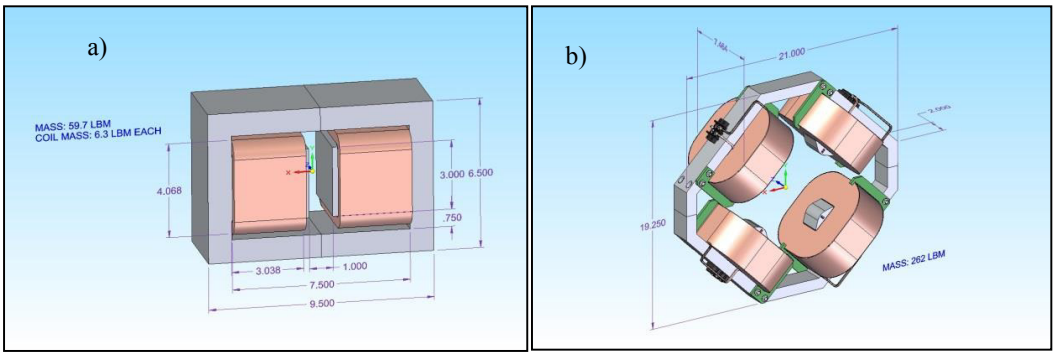

Fig. 3 (a) Beamline dipole and (b) quadrupole magnet

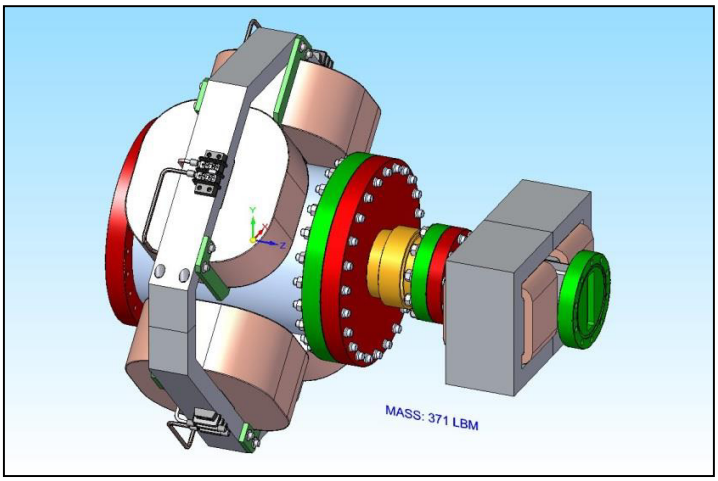

Figure 4: 3-D view of the beamline (beam comes in from the right)

For the quadrupole (see Fig. 3b), the desired full bore size is 20 cm (~8") and the pole tip field ~2000 G. This will be a dc magnet and it can thus have a solid iron core. Since longitudinal space is again very limited, we will limit the core steel length to 2 inches (5 cm), with a resultant effective magnetic length of ~10 inches (~25 cm). The generic magnetic designation will be an "8Q2" (i.e. a quadrupole with 8" bore and 2" core length). With a bore-to-length ratio of 4, this quadrupole will have non-negligible end effects. The quadrupole has a gradient of 200 G/cm for a pole tip field of 2000 G. The total number of ampere-turns to drive this flux will be of the order of 32,000, or 8,000 ampere-turns per pole. Using an excitation current of 16 A, each coil will need to have 500 turns. To minimize ohmic heating losses, we can use AWG #8 wire thickness and still have significant overhead left to drive the flux higher if needed. These coils and the ones for the dipole can be wound on the automatic coil winding machine already existing at SLAC. Fig. 4 shows an assembled picture of the whole beamline.

An example of the orbit for a 25° angle at the target, obtained using the MAD8 program (Grote, 2002), is shown in Fig. 5. Here, the kicker effective length is 10 cm, the quadrupole effective length is 15 cm, the distance between the kicker center and quadrupole center is 25 cm, and the total length of the beam transport line is estimated to be 50 cm. The target is located 15 cm downstream of the quadrupole center. A hard-edge quadrupole model is used in this example.

The beam vertical orbit in this system is linearly proportional to the angle at the target. The 55 mm orbit at a 25° angle requires a large quadrupole aperture which is comparable to the quadrupole length. Such a quadrupole is expected to have a significant fringe field extending beyond the effective length of the quadrupole. To assess sensitivity to the fringe field profile, three field models were studied, as shown in Fig. 6. These are the hard edge

model (as used in obtaining Fig. 5), where the gradient is constant over the quad length L; the linear fringe-1 model where the length of the constant gradient field is L / 2 and where the gradient diminishes linearly over length L / 2 at each end; and the linear fringe-2 model where the gradient diminishes linearly from the center of the quadrupole over length L at each end.

In order to assess sensitivity of the beam parameters at the target to the quadrupole field profile, these three optics models (i.e. “Hard edge”, “Linear fringe 1”, “Linear fringe 2”) were implemented into the Elegant code for beam tracking (Borland, 2000 and 2014). The Elegant code also calculates higher order effects generated by the fringe field. The calculated initial beam distributions at the end of the 270-degree magnet mentioned earlier were used for this simulation. The average energy of the beam distribution was 9.096 MeV with an energy spread of about ±1% (HWHM). The initial Gaussian RMS beam sizes are 0.324 mm in the (horizontal) x-plane and 0.637 mm in (vertical) y-plane. Since the quadrupole focuses in the y-plane and defocuses in the x-plane, it is beneficial that that the initial x-size is smaller, since it will increase at the target by the quadrupole defocusing effect.

The results of beam tracking are tabulated in Table 2 for the three models, corresponding to the maximum vertical angle at the target of 25°. The quadrupole gradient in each model was set for focusing the beam to x = y = 0 at the target. The resulting dependence of beam size on the model is rather weak, suggesting that a more realistic field model will produce very similar results. As expected, the x-size at the target is increased to 1.8-2.0 mm while the y-size is about 0.85 mm at the 25° angle. The vertical size has a contribution from momentum dispersion (generated by the kicker) which is proportional to the angle. Hence at a smaller angle, the y-size is smaller. In summary, the variation of the beam vertical position as a function of angle at the target is within 0.1 mm, and variation of beam x and y sizes at target is within 12% and 4%, respectively, for different fringe models. These variations are considered acceptable. The linearity of the relationship between the angles at the target versus the kicker strength is within 1%.

A magnetostatic analysis for the required system quadrupole focusing element was performed using the OPERA TOSCA magnetostatic analysis software package (Cobham 2014) in order to calculate higher order harmonics for the quadrupole. Effects of the individual quadrupole field harmonics on the beam vertical position at the target as a function of angle are obtained in MAD8 using the hard-edge quadrupole field model. The largest beam offsets (1-2 mm) correspond to the maximum 25° angle at the target and are produced by the largest harmonic contributions at n = 3 and 5. For angles < 20° the offsets are quickly reduced to well below 1 mm.

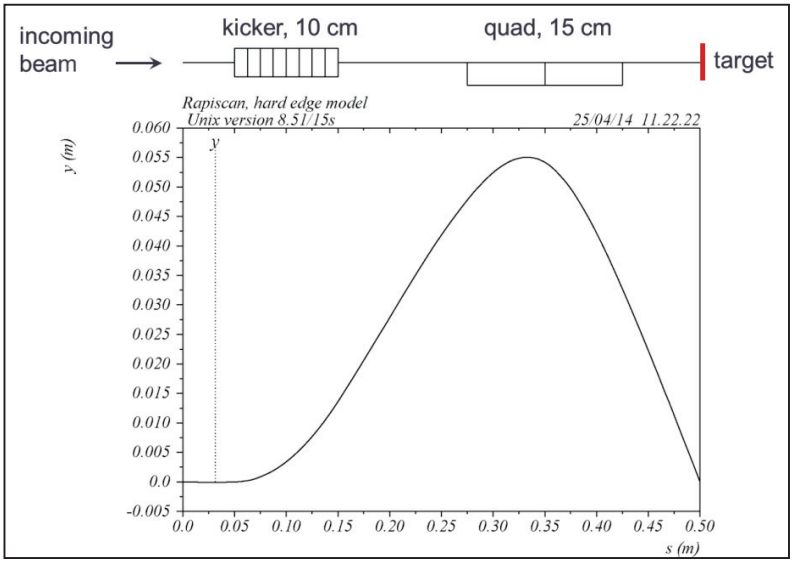

Fig. 5: Vertical orbit corresponding to 25° angle at target.

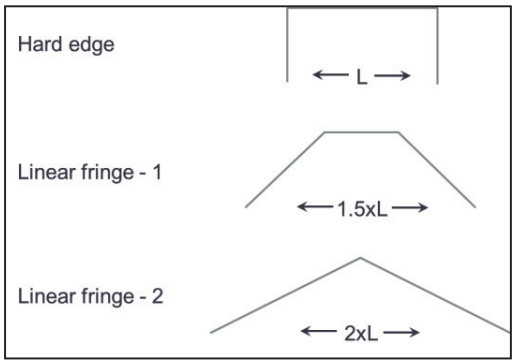

Fig. 6: Quadrupole field gradient models to study sensitivity to a fringe field profile.

Table 2: Beam size, position and angle at target as a function of quadrupole fringe model and desired angle at target.

		Hard edge		Linear fringe-1		Linear fringe-2	
Max. kicker BL (Gm)		81.3		82.4		85.5	
Quadrupole B'L (kG)		4.36		4.50		4.91	
Beam at target		**x**	**y**	**x**	**y**	**x**	**y**
Kicker set for -25° at target	σ (mm)	1.8	0.86	1.8	0.85	2.0	0.84
	position (mm)	0	0	0	0	0	0
	angle (degree)	0	–25.0	0	–25.0	0	–25.0
Kicker set for -12.5° at target	σ (mm)	1.8	0.53	1.9	0.53	2.0	0.54
	position (mm)	0	–0.10	0	–0.10	0	–0.12
	angle (degree)	0	–12.4	0	–12.4	0	–12.4
Kicker set for -6.25° at target	σ (mm)	1.8	0.46	1.9	0.46	2.0	0.48
	position (mm)	0	–0.06	0	–0.07	0	–0.08
	angle (degree)	0	–6.2	0	–6.2	0	–6.2

4. Truck-Mounted System

In order to move from the demonstration system to the truck-mounted system, the following approach was arrived at:

1. Engineer each component to meet mobile truck-mounted specifications.
2. Engineer the superstructure for support to be compact and as light as possible with emphasis on cooling and thermal stability for harsh environmental conditions such as IP65 (NEMA 2005) for water intrusion and dust penetration.
3. Optimize the 22-MV RF guide from the demonstration system to reduce the peak power from 3 MW to about 1 MW for a beam energy of 9 MeV with very low beam loading, and reduce the length of the accelerator so that it meets these requirements with a reasonable operating margin. The estimated length for this accelerator is approximately 1.1 m.
4. Optimize the cooling for the new guide specifically for the mobile application and its usage characteristics as well as for anticipated real-life environmental conditions. An S-band system, while not as small as an X-band system, would most likely meet the mobile platform requirements. The S-band platform has the largest number of available commercial components and the larger diameter and length of the components make them substantially easier to cool than X-band counterparts. The availability of S-band components also reduces the cost of the prototype system by at least 50%, based on current quotes for accelerator hardware.
5. Engineer the target. A comparison between a tungsten target and a carbon (diamond) target was performed. Known Varian Medical Systems target scaling properties for a tungsten target (proportional to $10^{2.7}$) and MCNPX models were used to determine the required currents for the desired dose rates, and from the

currents the expected beam loading was obtained. The beam loading for all cases is very low because the dose per pulse is extremely low, considering the 1 kHz pulse rate. Based on the radiative yields from NIST Estar (http://physics.nist.gov/PhysRefData/Star/Text/ESTAR.html), a scale factor of 20% for carbon relative to tungsten then yields the beam currents and loadings for a carbon target. A summary of the guide-specific parameters and the guide power budget is given in Table 3. Note that the beam power is negligible and the overall power budget is the same for both cases.

6. Design the RF network, circulator and load for mobile specifications. This includes resistance to shock and vibration, and any other specifications that exceed the requirements for the demonstration system.
7. The klystron can be de-rated, since in the demonstration system, the COTS klystron is essentially used at a lower power than it is designed for.
8. Because the goal of the demonstration system was to design a stable environment for testing rather than size, weight and layout, the bend magnet can be optimized and ruggedized, sized and positioned appropriately for the mobile application.
9. The temperature control unit for the demonstration system was also designed for continuous operation to fully test components. It can be optimized for both minimal size and power consumption because a mobile system would approximately have no more than a 50% beam-on time (scanning system duty factor). A larger cooling fluid reservoir than usually employed for mobile temperature stability can be used as a buffer and would have two cooling loops, as discussed before. Using two cooling loops should also reduce the overall cost for the cooling system.

Some of the components, such as the modulator, RF hardware, and gridded electron triode gun/driver would most likely remain the same as in the demonstration system. A sketch of the truck-mounted system is shown in Figure 7.

5. Summary

An agile mobile scanning system with reduced radiological footprint is highly desired. We have described a design of an accelerator and a vertically-scanning beam line optimized for such a system, and an approach to realizing the accelerator and the beam line in prototype form in two steps. We have shown that, in a first step, existing components can be used with some modifications and assembled into a demonstration system that provides a stable platform for testing. Optimizing and engineering the components for mobile applications would be performed in a second step. Parmela accelerator beam transport calculations were performed for various demonstration system configurations and used in a design of beam line dipole and quadrupole magnets. A concept of an industrial K15 system housing with relevant modifications for the demonstration system was described, and the engineering tasks for the truck-mounted evolution of the system were given.

Table 3 Truck-mounted system guide-specific parameters and power budget

	Target: Tungsten	**Carbon**	
Beam Energy	9	9	MeV
Max Dose Rate @ 100 cm	100	100	Rad/(min)
Rep Rate	1000	1000	Hz
Average Beam Current	3.8	18.9	μA
Peak Current	378.8	1,890	μA
Electrons/pulse	2.40E+10	1.18E+11	
Average Beam Power	34.1	170.5	W
Peak Beam Power	3.4	17.0	kW
Charge/Pulse	3.8	18.9	nC
Shunt Impedance	100	100	MΩ/m
Estimated Accelerator Length	1.1	1.1	m
RF Power Cavities	0.89	0.89	MW
Reflected Power	0.089	0.089	MW
Average Beam Power	3.40E-05	1.70E-04	MW
Total Power (Estimated)	**0.980**	**0.980**	**MW**

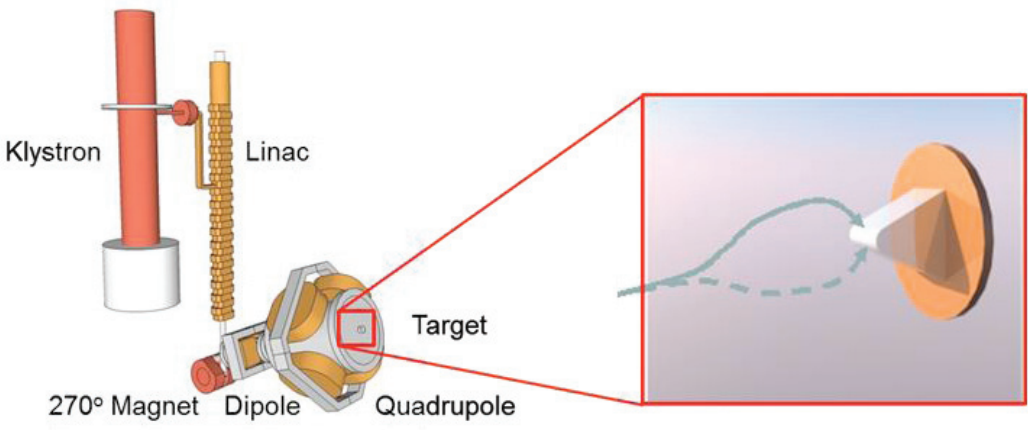

Fig. 7: A sketch of the klystron, guide, bend magnet and fan-beam steering beam line.

Acknowledgements

This work has been supported by US Department of Homeland Security, Domestic Nuclear Detection Office, under competitively awarded contract HSHQDC-14-C-B0002. This support does not constitute an express or implied endorsement on the part of the Government.

References

Borland, M. 2000, "Elegant: A Flexible SDDS-Compliant Code for Accelerator Simulation," Argonne Advanced Photon Source (APS) Tech. Rep. LS-287.

Borland, M., 2014., "User's Manual for elegant," http://www.aps.anl.gov/Accelerator_Systems_Division/Accelerator_Operations_Physics/manuals/elegant_latest/elegant.html.

Cobham 2014, OPERA 3D software, Cobham Technical Services Vector Fields Inc.,1700 N Farnsworth Ave, Aurora IL 60505, http://www.cobham.com.

Condron, C., Brown, C., Gozani, T., Hernandez, M., Langeveld, W.G.J. 2013, "Linear Accelerator X-Ray Sources with High Duty Cycle", AIP Conf. Proc. 1525 pp. 704.

Grote, H. 2002, http://hansg.home.cern.ch/hansg/mad/mad8/mad8.html, and MADX, http://frs.web.cern.ch/frs/Xdoc/mad-X.html.

Langeveld, W.G.J., Condron, C., Elsalim, M., and Ingle, M. 2011, "Noise Spectroscopy: Z-determination by Statistical Count-rate ANalysis (Z-SCAN)", Nucl. Inst. Meth. A 652 pp. 79.

Langeveld, W.G.J., Condron, C., Elsalim, M., Grudberg, P., Hu, V., Ryge, P., Shaw, T., and Sinha, S. 2013, "Implementation of Noise Spectroscopy using biased large-area photodiodes", IEEE Trans. Nucl. Sc., 60 pp. 937.

Langeveld, W.G.J., Gozani, T., Ryge, P, Sinha, S., Shaw, T., and Strellis, D. 2013, "A Whole-System Approach to X-Ray Spectroscopy in Cargo Inspection Systems", AIP Conf. Proc. 1525 pp. 690.

Langeveld, W.G.J., Johnson, W.A., Owen, R.D., and Schonberg, R.G. 2009a, "Intensity Modulated Advanced X-ray Source (IMAXS) for homeland security applications(I)", IEEE Trans. Nucl. Sc., 56 pp. 1288.

Langeveld, W.G.J., Johnson, W.A., Owen, R.D., and Schonberg, R.G. 2009b, "Intensity Modulated Advanced X-ray Source (IMAXS) for homeland security applications(II)", AIP Conf. Proc. 1099 pp. 628.

Langeveld, W.G.J., Brown, C., Christensen, P.A., Condron, C., Hernandez, M., Ingle, M., Johnson, W.A., Owen, R.D., Ross R., and Schonberg, R.G. 2011, "Performance characteristics of an Intensity Modulated Advanced X-ray Source (IMAXS) for homeland security applications", AIP Conf. Proc. 1336 pp. 705.

NEMA 2005, https://www.nema.org/Products/Documents/nema-enclosure-types.pdf.

Sinha, S., Kwong, J., Langeveld, W.G.J., and Ryge, P. 2013, "Characterization of ZnO, BaF2 and PbWO4 scintillator detectors for cargo inspection using transmitted x-ray spectroscopy", IEEE Trans. Nucl. Sc., 60 pp. 1016.

Stevenson, J., Gozani,T., Elsalim, M., Condron, C., Brown, C. 2010, "Linac based photofission inspection system employing novel detection concepts", Nucl. Instrum. Meth. Phys. Res. A, vol. 652 pp. 124-128.

Young, L. M., 2003, PARMELA, Los Alamos National Laboratory report LA-UR-96-1835 (Revised April 22, 2003).